

A new floating Energy Storage System based on Fabric

Robert Klar*, Bernd Steidl and Markus Aufleger

*Unit of Hydraulic Engineering, Faculty of Engineering Science, University of Innsbruck
Technikerstraße 13, 6020 Innsbruck, Austria*

Abstract

This paper focuses on the theoretical investigation of the 'light' version of the Buoyant Energy (BE) storage concepts. Generally, BE transfers the pumped-storage hydropower key features to an offshore environment. The 'light' BE version is characterized by a lower water level of the surrounding water compared to the inner water level of the energy storage device. Therefore, it benefits from light construction material. Maybe the most lightweight construction method is the use of waterproof fabric material. First, the basic design aspects and ideal storage capacities of the original 'light' BE concept using rigid reservoirs is assessed. Second, a new design approach based on fabric is introduced. After describing and discussing its main components, the underlying equations are applied to form an exemplary energy storage device with 5 MWh capacity. Third, a design approach for increasing the energy storage capacity of airproof 'light' BE systems by added air compression to increase the pump-turbine head is presented. Fourth, floating stability aspects of 'light' BE devices are highlighted based on two exemplary box shaped design. The results indicate that the ideas for using fabric as a construction material are promising and should be subject to further studies.

1. Introduction

1.1 Background

The need of more energy storage capacity to compensate imbalanced supply and demand in future renewable energy grids is widely undoubted. Therefore, several storage systems are under development and compete with each other. Promising examples are the Tension Leg Platform integrated Hydraulic Accumulator [1], the StEnSea subsea energy storage technology [2], Ocean Renewable Energy Storage [3], Energy Bags for underwater Compressed Air Energy Storage (CAES) [4] and Constant Pressure Accumulators for Offshore Wind Turbines [5].

Buoyant Energy (BE) [6] is a floating hydraulic energy storage system. In essence, it consists of large and floating reservoirs and hydraulic pump-turbine/motor-generator systems for energy conversion. In a charge-discharge cycle, electrical power is converted to gravitational energy and back again. BE is suitable for nearshore and offshore storage needs and uses the well-established technology of pumped-storage hydroelectricity (PSH) in a new arrangement.

The ongoing exploratory project 'PrepareBE' [7], which started in January 2017, aims to clarify its technical feasibility and economic viability. Furthermore, the project determines the most promising application fields and defines development goals with the best chances of success. Buoyant Energy benefits from its simple architecture and high adaptability to local boundary conditions. It provides unlimited number of load cycles, short response times, high operation efficiency and multi-use space on the platform roof and inside the structure for e.g. wind farm operation, transport, industry, leisure, accommodation or aquaculture.

1.2 Basic 'Light' BE Concept

One of the BE concepts is characterized by a lower water level of the surrounding water compared to the inner water level of the floating energy storage device. For this purpose, a fluid reservoir is equipped with buoyant bodies as shown in Figure 1. In turbine operation mode water flows from the fluid reservoir to the surrounding water, driving a turbine. The floating energy storage platform rises and the stored gravitational energy is converted into electric energy. In pump operation mode the floating structure moves down, thereby converting electric energy into potential energy and storing it. A lightweight construction is advantageous compared to the use of heavy materials for a platform structure. Therefore it is called the 'light' version of BE.

*Corresponding author, robert.klar@uibk.ac.at

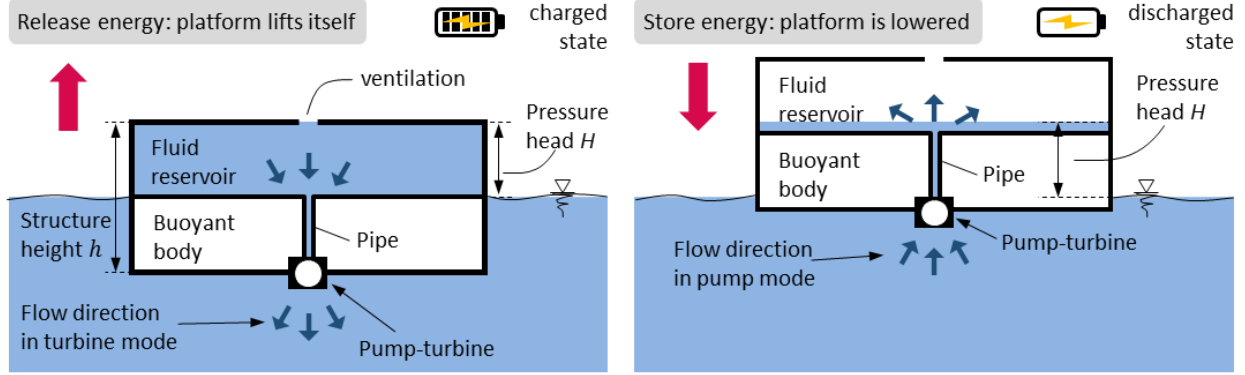


Figure 1. Schematic sketch of the 'light' version of Buoyant Energy in charged (left) and discharged (right) state.

1.3 Basic Design Aspects and Ideal Storage Capacity

The 'light' BE version benefits from light construction material, which could result in significantly reduced investment costs compared to the 'heavy' BE solution [6]. The use of flexible fabric material could be a potential option and is discussed in chapter 2. Due to the relatively high elevation of the centre of gravity compared to the center of buoyancy, the floating stability especially in bad weather and sea conditions has to be considered carefully (chapter 4). Therefore, low and wide structures providing sufficient form stability could be favourable.

The useable energy content of a 'light' BE energy storage system depends upon the shape of its fluid reservoir, buoyant body and its mass (structure, technical equipment). An idealized BE system (Figure 1 and 2) is used to show the functional relationship. Fluid reservoir and buoyant body are shaped cylindrically and share the same base area A . The wall thicknesses t are considered infinitely thin. Figure 2 shows three schematic sketches of ideal BE devices each one with different fluid reservoir volumes $V_{A,i}$ and heights $h_{A,i}$, buoyant body volumes $V_{B,i}$ and heights $h_{B,i}$ and pressure heads H_i .

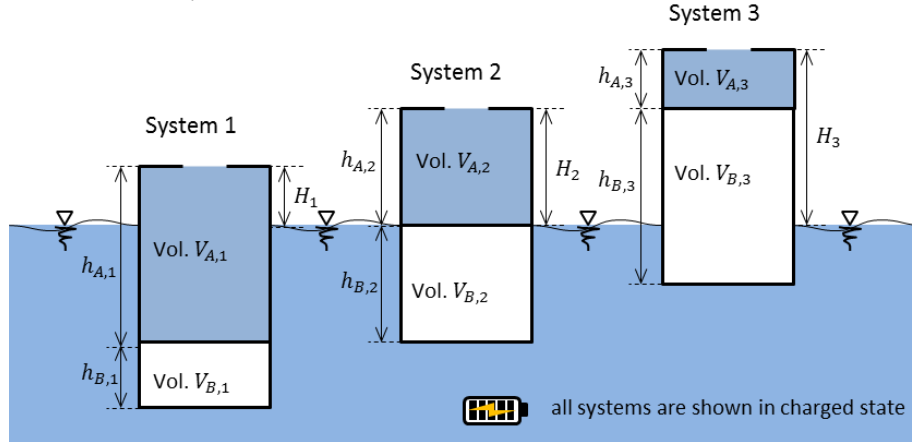


Figure 2. Schematic sketches of three 'light' BE systems with the same structure height h and base area A but different fluid reservoir and buoyant body volumes (pump-turbine and technical equipment is not shown).

The following equations 1 to 5 describe boundary conditions and functional relationships, which characterize such ideal BE storage systems. The used equation symbols are the water density ρ_w , the gravitational acceleration g , the pressure head H , the flow rate Q , the filling time t_{max} , the power P and the energy storage capacity W .

$$A = const. \quad | \quad Q = const. \quad | \quad h = h_A + h_B = const. \quad (1)$$

$$V_A + V_B = A \cdot h = A \cdot (h_A + h_B) \quad \text{with} \quad V_A = A \cdot h_A \quad \text{and} \quad V_B = A \cdot h_B \quad (2)$$

$$t_{max} = V_A / Q \quad | \quad H = h - h_A = h_B \quad (3)$$

$$P = \rho_w \cdot g \cdot H \cdot Q \quad (4)$$

$$W(t_{max}) = P \cdot t_{max} = \rho_w \cdot g \cdot H \cdot V_A = \rho_w \cdot g \cdot (h - h_A) \cdot A \cdot h_A \quad (5)$$

For each BE system of Figure 2 the specific storage capacity can be calculated according to equation 5. The ‘optimal’ height $h_{A,opt}$ to maximise the energy capacity $W(t_{max})$ for a given structure height h and base area A is derived from the following equation:

$$dW/dh_A = 0 \rightarrow h - 2 \cdot h_{A,opt} = 0 \rightarrow h_{A,opt} = h/2 \quad (6)$$

As a result, the storable energy content reaches its maximum, if the fluid reservoir and buoyant body heights are equal to the half structure height h and the pressure head H (equation 7). The ‘optimal’ energy capacity $W_{opt}(t_{max})$ of an idealized ‘light’ BE system is expressed by equation 8 and illustrated in Figure 3.

$$h_A = h_B = h/2 = H \quad (7)$$

$$W_{opt}(t_{max}) = \rho_w \cdot g \cdot A \cdot h^2/4 = m \cdot g \cdot h/2 \quad (8)$$

The volumetric energy density ρ_{vol} related to the volume of displaced in fully charged state is:

$$\rho_{vol} = W_{opt}/V_B = W_{opt}/(A \cdot h_B) \quad (9)$$

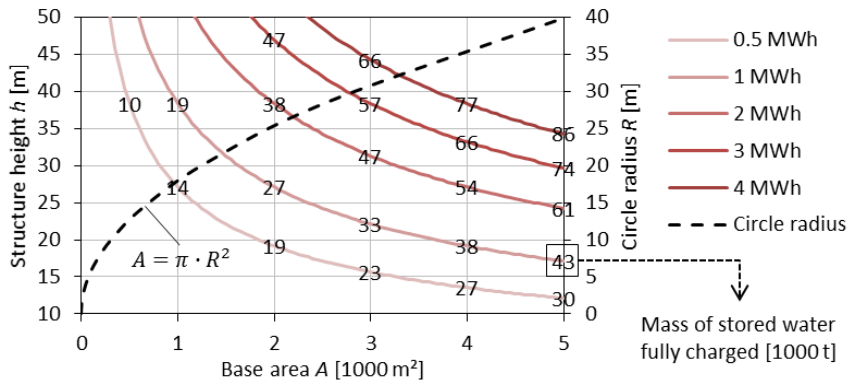


Figure 3. ‘Optimal’ Energy storage capacity as a function of structure height h and the base area A .

2. Design Approach for a Floating Energy Storage System based on Fabric

2.1 Proposed New Concept

Maybe the most lightweight construction method to build up a ‘light’ version BE storage device is the use of waterproof fabric material. The development of BE structures composed of fabric is on a very early stage. The intention of the following design approach is to show its principal feasibility and to get indications for possible dimensions and associated energy storage capacities. The main motivation to find storage solutions based on fabric is an expected decrease of construction costs compared with rigid structures and advantages for fabrication, packaging, shipment and deployment.

Figure 4 presents the first design approach and shows two main components:

- (1) The stabilizing structure: Several stabilizing fabric tubes are arranged to form a ring-like tubular structure supported by buoyant bodies. Because the water inside the airproof tubes is at higher pressure than at the outside, they act as beams and provide resistance against bending. Each tube is attached to a fabric membrane at the inside. The stabilizing structure forms a large and considerably rigid vertical tube.
- (2) A new ‘light’ BE storage system with expandable fabric walls: A big waterproof fabric tube with circular cross-section and filled with water floats inside the stabilizing structure. It consists of a floating brim with flexible, foldable or collapsible fabric walls. A buoyant body forms the lower end of the tube and causes a water level difference (pressure head) between inside tube and outside sea. In turbine operation mode water flows from the tube to the surrounding water and the buoyant body moves up. The flexible fabric tube walls wrinkle or fold in vertical direction. Due to the expandable nature of the walls, the pressure head maintains a constant level difference. The tube’s water surface level will be the same, regardless of the reservoir’s fill level. In pump operation mode water is moved from the surrounding water to the tubular flexible reservoir. The pumped water is stored below the water’s surface and causes a downward movement of the buoyant body. The waterbody inside the flexible tube is open for a multipurpose use like open-ocean-aquaculture.

The geometries of the two main components (1) and (2) depend functionally on each other. The ratio R/r and the maximum cross-section diameter d_{max} of the ‘light’ BE storage system is described in equation 10 with R the circumscribed circle of the ring-like tubular structure, r the inner radius of each stabilizing tube and k the number of stabilizing tubes enclosing the ‘light’ BE system.

$$R/r = 1 + 1/\sin(\pi / k) \quad | \quad d_{max} = 2 \cdot R - 4 \cdot r \quad (10)$$

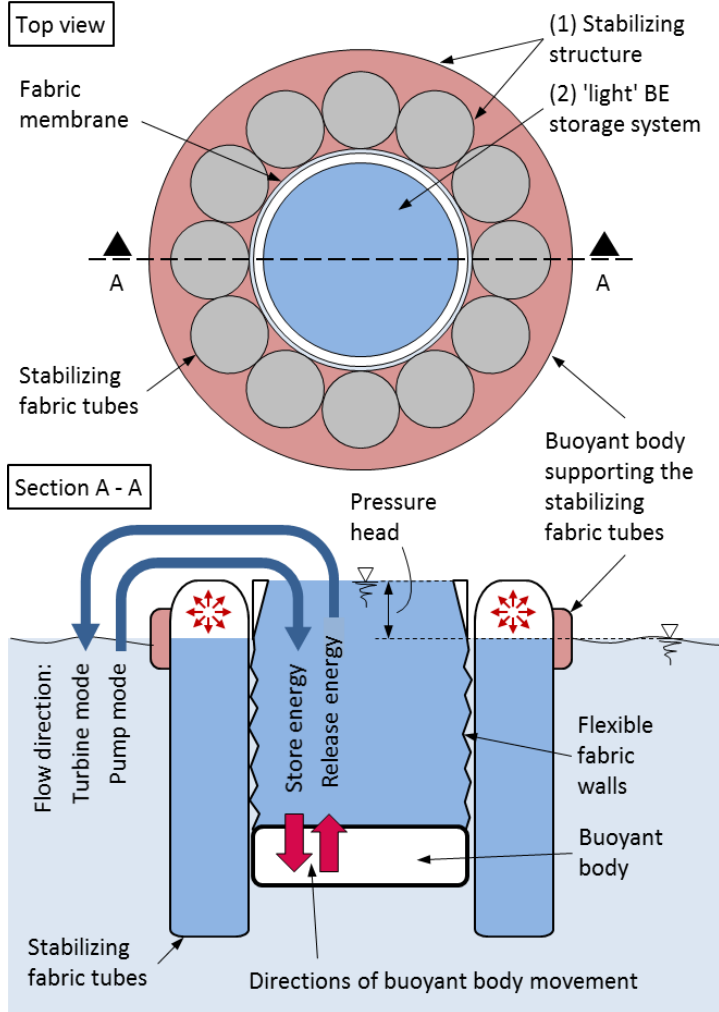


Figure 4. Schematic sketch of the ‘light’ version of BE, based mainly on fabric material (pump-turbine and technical equipment is not shown).

2.2 ‘Light’ BE Storage Architecture with Expandable Fabric Walls

Figure 5 shows the ‘light’ version of BE with expandable fabric walls (main component 2 in chapter 2.1) as a reduced schematic sketch in discharged and charged state. The following equations 11 characterize some design parameters and equation 12 defines the storage capacity $W_{BE,A \rightarrow B}$ of such an ideal BE system. All parameters and mathematical symbols used within the following equations are listed in Table 1.

$$V = A \cdot h_A \quad | \quad p_A = \rho_w \cdot g \cdot h_A + p_0 \quad | \quad p_B = \rho_w \cdot g \cdot h_B + p_0 \quad | \quad H = h_A \quad (11)$$

$$W_{BE,A \rightarrow B} = \eta_{BE} \cdot \rho_w \cdot g \cdot (h_B - h_A) \cdot A \cdot H = \eta_{BE} \cdot \rho_w \cdot g \cdot (h_B - h_A) \cdot A \cdot h_A \quad (12)$$

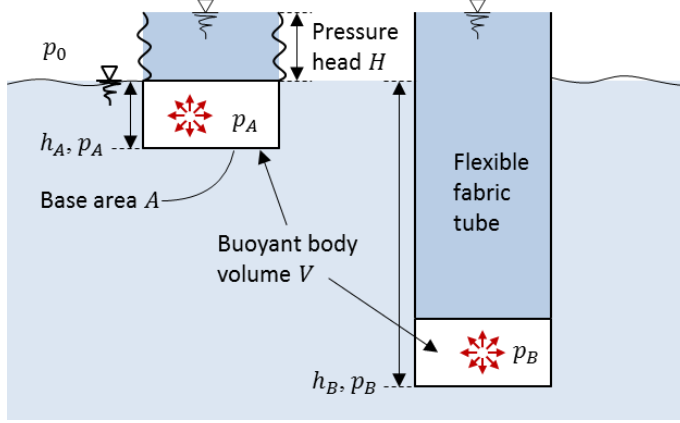


Figure 5. Schematic sketch of the ‘light’ version of BE with expandable fabric walls in discharged (left) and charged (right) state (pump-turbine and technical equipment is not shown).

The buoyant body bears the potential for additional compressed air energy storage. If it would be made of fabric and would be lowered by inflowing water from the BE pump operation, then the pressure of the surrounding seawater would increase and the volume of the buoyant body would decrease. As a result, the buoyant body would lose its shape and the buoyancy force and pressure head H would decrease. Hence, it is necessary to ensure a constant buoyant body volume either by rigid boundaries or by a dynamical adapted inside air pressure. This means from a thermodynamic point of view, that this system is a constant volume and variable pressure system. For isothermal air compression and expansion, the resulting ideal compressed air energy storage capacity $W_{CAES,A \rightarrow B}$ is:

$$W_{CAES,A \rightarrow B} = \eta_{CAES} \cdot \Delta p_{A \rightarrow B} \cdot V = \eta_{CAES} \cdot (p_B - p_A) \cdot V = \eta_{CAES} \cdot \rho_w \cdot g \cdot (h_B - h_A) \cdot A \cdot h_A \quad (13)$$

The total energy storage capacity W_{sum} is for system efficiency's $\eta_{BE} = \eta_{CAES} = 1$ the doubled BE capacity $W_{BE,A \rightarrow B}$.

$$W_{sum} = W_{BE,A \rightarrow B} + W_{CAES,A \rightarrow B} = \rho_w \cdot g \cdot A \cdot (h_B - h_A) \cdot h_A \cdot (\eta_{BE} + \eta_{CAES}) \quad (14)$$

The volumetric energy density related to the volume of displaced water is:

$$\rho_{vol} = W_{sum}/V = W_{sum}/(A \cdot h_A) \quad (15)$$

Table 1 presents the application of equation 11 to 15 for exemplary BE parameters and shows the results.

Table 1. Parameters and results for an exemplary ‘light’ BE storage architecture with expandable fabric walls.

Parameter	Value	SI unit
Cross-section diameter ‘light’ BE storage system d	32	m
Base area $A = d^2/4 \cdot \pi$	804,2	m ²
Pressure head H	15	m
Volume of stored water $V = (h_B - h_A) \cdot A$	15000	m ³
System efficiency's $\eta_{BE} = \eta_{CAES}$	1	-
Atmospheric pressure p_0	1,01	bar
Height of buoyant body h_A	15	m
Maximum immersion depth h_B	90	m
Pressure p_A at depth h_A	2,48	bar
Pressure p_B at depth h_B	9,84	bar
Differential pressure $\Delta p_{A \rightarrow B}$	7,36	bar
Storage capacity, solely ideal BE system $W_{BE,A \rightarrow B}$	2,47	MWh
Storage capacity, solely ideal CAES system $W_{CAES,A \rightarrow B}$	2,47	MWh
Storage capacity, total W_{sum}	4,93	MWh
Volumetric energy density ρ_{vol}	0,41	kWh·m ⁻³
Thickness t of the flexible fabric tube walls	10	mm
Stress in circumferential direction $\sigma_\theta = (h_A \cdot \rho_w \cdot g \cdot d)/(t \cdot 2)$	235	MPa
Stress in longitudinal direction σ_x	0	MPa

Figure 6 uses the exemplary parameters of Table 1 and shows the effects of varying geometric properties on the stored energy capacity.

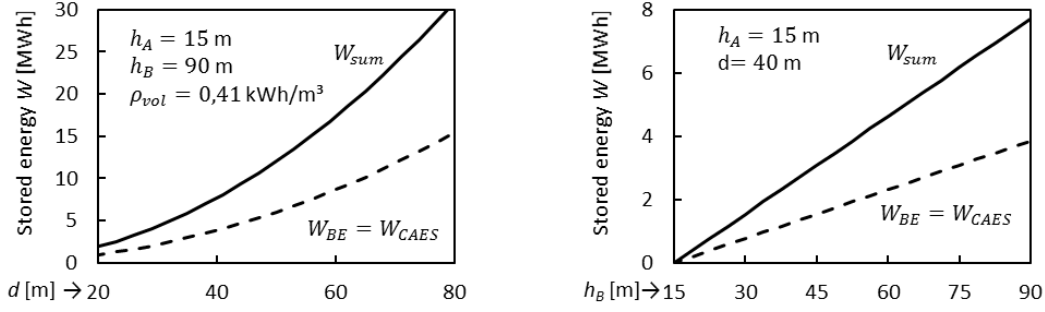


Figure 6. Stored energy contents for varying diameter d and maximum immersion depth h_B .

2.3 Stabilizing Structure based on Fabric

Veldman [9] gives an excellent overview of applications of inflatable structures and associated technologies. In general, inflatable structures offer advantages such as being lightweight and simple to deploy. Additionally they have a high packaging efficiency, which is important for transport purposes. These advantages are incorporated in many applications like air-supported or air-inflated structures, dual wall structures or inflatable beams. However, floating stabilizing structures based on fabric as introduced in chapter 2.1, Figure 4 and 7 seem to be a not yet pursued idea. A stabilizing tube consists of water- and airtight fabric with circular cross-section that floats in the sea and is filled with water (Figure 4 and 7). On the top side of the tube there is a gas volume and provides an internal pressure $p > p_0$. Several stabilizing fabric tubes form a ring-like tubular structure and are supported by buoyant bodies. This architecture ensures a kind of fixed support for each tube at the water surface. Each tube acts as beam and therefore provides resistance against bending and shear force. A simplified static model is shown in Figure 7.

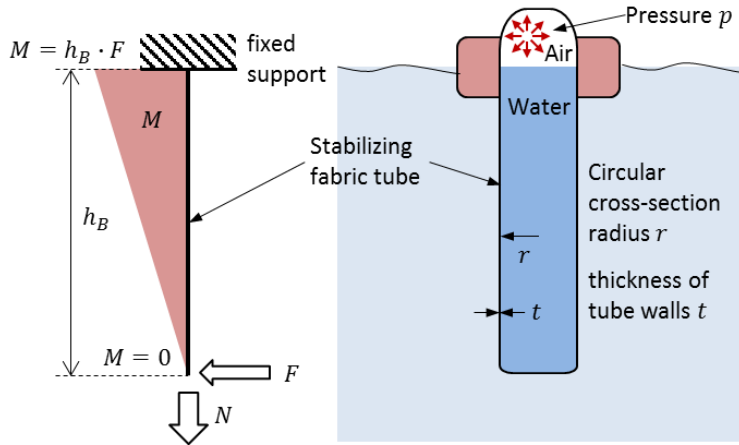


Figure 7. Simplified static model of one stabilizing fabric tube.

The equilibrium of forces and moments gives (with normal force N , moment M , radius r , shear load F at depth h_B):

$$\sum N = 0: N = p \cdot \pi \cdot r^2 = t \int_0^{2\pi} \sigma_x \cdot r \, d\theta \quad (16)$$

$$\sum M = 0: M = h_B \cdot F = -r^2 \cdot t \int_0^{2\pi} \sigma_x \cdot \cos \theta \, d\theta \quad (17)$$

In an unwrinkled situation the stress distribution due to pressurisation p and shear load F will be as follows [10] (with the stresses σ_x in longitudinal and σ_θ in the circumferential direction and the shear stress $\tau_{x\theta}$):

$$\sigma_x = N/A_{tube} - (M \cdot r \cdot \cos \theta)/I_{xx} = (p \cdot r)/(2 \cdot t) - (M \cdot \cos \theta)/(\pi \cdot r^2 \cdot t) \quad (18)$$

$$\sigma_\theta = (p \cdot r)/t \quad (19)$$

$$\tau_{x\theta} = -(F \cdot \sin \theta)/(\pi \cdot r \cdot t) \quad (20)$$

The bending moment at which collapse takes place is defined as the moment at which an increase in deflection does not result in an increase in moment. A good overview of several different expressions for calculating the collapse moment is summarized by Veldman et al. [9]. The collapse moment according to Wielsgosz et al. [11] is a function of the internal pressure p and the cross-section radius r :

$$M_{Wielsgosz} = \left(\frac{\pi}{2}\right)^2 \cdot p \cdot r^3 \quad (21)$$

At the wrinkling pressure $p_{wrinkling}$ a first local wrinkle appears. Since the stabilizing fabric tube is made of a membrane, the internal pressure p should always be higher than $p_{wrinkling}$ which is described by equation 22 according to Le van et al. [12].

$$p_{wrinkling} \geq F \cdot (2 \cdot h_B) / (\pi \cdot r^3) \quad (22)$$

The stabilizing fabric tubes are attached to each other and to a fabric membrane at the inner side. This will add considerably to the stability of the structure but is not taken into account in this preliminary design study. All together, the stabilizing structure forms a ring-like tubular structure. As a consequence, the movement of the buoyant body of the 'light' BE storage system inside the tubular structure is free in vertical but locked in lateral direction.

Table 2 shows the parameters and results for an exemplary stabilizing structure consisting of $k = 12$ stabilizing fabric tubes. The new 'light' BE storage system with expandable fabric walls and a cross-section diameter $d = 32$ m described in chapter 2.2 and Table 1 perfectly fits into it. One tube can resist a shear load of $F = 1500$ kN at a depth of $h_B = 90$ m. The total resistance will be higher than $F \cdot k = 18$ MN due to the architecture of the entire stabilizing structure. Further investigations have to clarify if the overall resistance is good enough to prevent the buoyant body of the 'light' BE storage system from moving laterally or from twisting inside the tubular stabilizing structure.

Table 2. Parameters and results for a stabilizing structure based on fabrics.

Parameter	Value	SI unit
Radius r of the stabilizing tube	5,7	m
Number k of stab. tubes enclosing the BE system	12	-
Circumscribed circle radius R according to equation 10	27,7	m
Maximum BE diameter d_{max} according to equation 10	32,6	m
Thickness t of the fabric tube walls	10	mm
Pressure $p = 5 \cdot p_0$	5,07	bar
Stress in the circumferential direction σ_θ	289	MPa
Shear load F (according to Figure 7)	1500	kN
Depth h_B (= application point of load F)	90	m
Moment $M = h_B \cdot F$ at the fixed support position	135000	kNm
Stress in the longitudinal direction $\sigma_x(\theta = 0)$	12	MPa
Stress in the longitudinal direction $\sigma_x(\theta = \pi)$	277	MPa
Shear stress $\tau_{x\theta}$	8	MPa
Collapse moment $M_{Wielsgosz} > M$ (equation 21)	231500	kNm
Wrinkling pressure $p_{wrinkling} < p$ (equation 22)	4,64	bar

2.4 Suitable Flexible Material

A suitable material needs to be strong, in order to cope with the design stresses and loads. It also needs to be durable and should not degrade in its characteristics even after years of seawater and sun exposure. Pimm et al. [4] specified some requirements to be considered for their Energy Bag technology [4]. In essence these requirements can be applied as well for Buoyant Energy architectures. A fabric structure must be as follows:

- Be structurally determinate and performance-predictable.
- Be resilient enough to retain its mechanical properties throughout fabrication, packaging, shipment, deployment, servicing and the intended long-term charging/discharging cycling regime.
- Be of sufficiently high specific strength to resist all stresses with enough margins of safety.
- Be biologically inert over its anticipated service life.
- Remain highly impermeable to pressurised water (and air) throughout the anticipated service life.

- Expandable fabric wall material in fully charged and unfolded state (Figure 5, right side) have to be foldable or collapsible into a suitable compact arrangement in the brim of the fluid reservoir when the reservoir is in discharged state (Figure 5, left side).

Pimm et al. [4] used for the prototype design of their Energy Bag 420d polyurethane-coated Nylon for the bladder and Vectran™ for the tendons. Future research has to clarify what kind of suitable material fits best for the proposed floating energy storage system based on Fabric (chapter 2). The following table lists some suitable materials regarding the ultimate tensile strength, which is above the needed limits of Table 1 and 2 with enough margins of safety.

Table 3. Tensile strength for selected materials.

Material	Tensile strength [GPa]
Vectran™ NT	1,1
Vectran™ HT	3,2
Glass fibre	~3,4
Carbon fibre	~4,1

3. Design Approach to Increase the Energy Storage Capacity

The design approach is an expansion of the basic 'light' BE system (chapter 1.2) to a hydro-pneumatic storage device. Compared to the BE approach additional energy is stored by compressing air in pump mode in chamber A and B (Figure 8). Therefore, the air volumes in chambers A and B have to be airproof and are designed with an umbilical connection as shown in Figure 8. Energy is released by air expansion acting on the liquid piston in chamber A. The whole process is modeled isothermal. Hence, the air in the system is kept at a constant temperature throughout. This necessarily requires exchange of heat with the water inside chamber A and the surrounding sea. The aim of this chapter is a first estimation of the consequences under ideal circumstances for the pump-turbine head H_{PT} and power P , which are no longer time invariant. Furthermore, the possible increase in storage capacity is shown. All system parameters and mathematical symbols used within the following equations are described in Table 4.

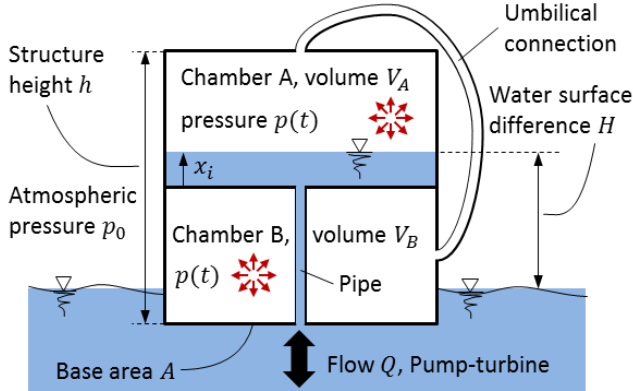


Figure 8. Schematic sketch of an airproof 'light' BE system with umbilical connection between its chambers.

The following equations 23 describe the boundary conditions for this estimation.

$$H = h/2 = const. \quad | \quad Q = const. \quad | \quad V_A = V_B \quad | \quad Q \cdot t_{max} = V_A \quad | \quad x_i \cdot A = t \cdot Q \quad (23)$$

The initial pressure in chamber A and B shall be p_{pre} . The ideal gas law for the assumed isothermal process leads to a functional relationship to express the time invariant air pressure $p(t)$ (equations 24 and 25).

$$p_{pre} \cdot (V_A + V_B) = p(x_i) \cdot (V_A + V_B - x_i \cdot A) = p(t) \cdot (V_A + V_B - t \cdot Q) \quad (24)$$

$$p(t) = p_{pre} \cdot \left(\frac{1}{1 - \frac{t \cdot Q}{V_A + V_B}} \right) \quad (25)$$

Bernoulli's equation describes the time invariant pump-turbine head $H_{PT}(t)$:

$$\frac{p_0}{\rho_w \cdot g} + H_{PT} = H + \frac{p(t)}{\rho_w \cdot g} \quad (26)$$

$$H_{PT}(t) = H + \frac{p(t) - p_0}{\rho_w \cdot g} = H + \frac{1}{\rho_w \cdot g} \cdot \left[p_{pre} \cdot \left(\frac{1}{1 - \frac{t \cdot Q}{V_A + V_B}} \right) - p_0 \right] \quad (27)$$

Finally, the power $P(t)$ and the energy storage capacity or work $W(t)$ can be calculated at any time $0 \leq t \leq t_{max}$:

$$P(t) = \rho_w \cdot g \cdot Q \cdot H_{PT}(t) = \rho_w \cdot g \cdot Q \cdot \left\{ H + \frac{1}{\rho_w \cdot g} \cdot \left[p_{pre} \cdot \left(\frac{1}{1 - \frac{t \cdot Q}{V_A + V_B}} \right) - p_0 \right] \right\} \quad (28)$$

$$W(t) = \int P dt = \rho_w \cdot g \cdot V_A \cdot H + V_A \cdot \left(p_{pre} \cdot \frac{2 \cdot (-\ln 0,5)}{1,38629} - p_0 \right) \quad (29)$$

Table 4 presents the application of equation 23 to 29 for exemplary BE parameters and shows the results.

Table 4. Parameters and results for an exemplary airproof 'light' BE system with umbilical connection between its chambers according to Figure 8.

Parameter	Value	SI unit
Water surface difference H	15	m
Structure height h	30	m
Base area A	1000	m ²
Volume $V_A = V_B = H \cdot A$	15000	m ³
Atmospheric pressure p_0	1,01	bar
Pre-charge pressure p_{pre}	10,13	bar
Flow rate pump-turbine Q	5	m ³ /s
Filling time t_{max}	3000	s
Pressure $p(t = 0) \mid p(t_{max})$	10,13 \mid 20,27	bar
Head pump-turbine $H_{PT}(t = 0) \mid H_{PT}(t_{max})$	108 \mid 211,2	m
Power pump-turbine $P(t = 0) \mid P(t_{max})$	5,29 \mid 10,36	MW
Storage capacity with compressed air $W(t_{max})_{CA}$	6,04	MWh
Storage capacity without compression $W(t_{max})_{BE}$	0,61	MWh

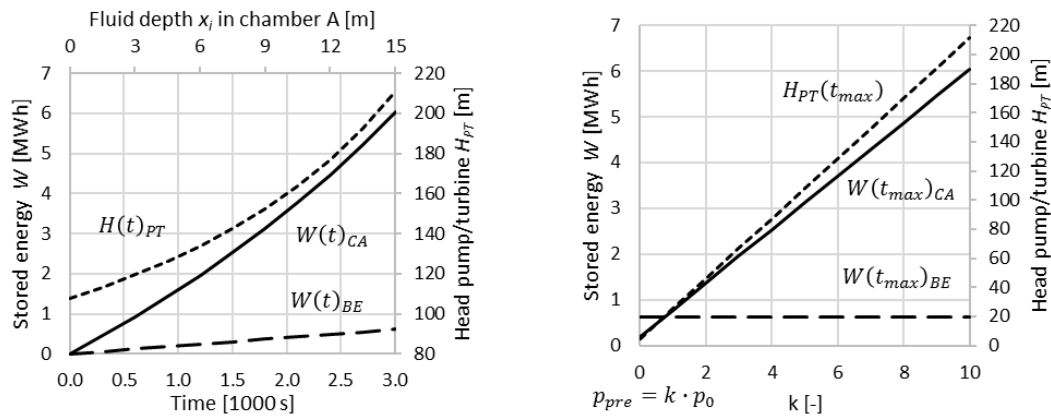


Figure 9. Diagrams illustrating the time course and the effects of pre-charge pressure p_{pre} on selected parameters for the exemplary system according to Table 4.

The ratio $W(t_{max})_{CA}/W(t_{max})_{BE} = 9,86$ describes the benefit of the design approach in comparison to a basic 'light' BE system. The increase of energy storage capacity goes hand in hand with a large difference in power and head values along the charging process. The left diagram of Figure 9 presents the non-linear increase of head $H_{PT}(t)$ with charging time t . The right diagram of Figure 9 shows the effect of a varying pre-charge pressure p_{pre} on the head $H_{PT}(t_{max})$ and the storage capacity with compressed air $W(t_{max})_{CA}$.

4. Floating Stability Aspects of Basic 'Light' BE Devices

The most important design characteristic of a floating BE storage device is to guarantee the floating stability for all fill levels k from 0 to 100 %. In order to assess the static floating stability (Figure 10), the resulting forces F , the righting moment M_y and righting arm RA_y can be expressed by equations 30 to 33. The application points of the vertical forces depend on the selected tilt angle α .

$$F_{Buoyancy} = F_{Structure} + \sum_i F_{Water,i} \quad (30)$$

$$F_{Water,i} = \rho_w \cdot V_{Water,i} \cdot k \cdot g \quad (31)$$

$$M_y = F_{Structure} \cdot (x_{Structure} - x_{Buoyancy}) + \sum_i F_{Water,i} \cdot (x_{Water,i} - x_{Buoyancy}) \quad (32)$$

$$RA_y = M_y / F_{Buoyancy} \quad (33)$$

Hydrodynamic forces and moments arising from dynamic sloshing effects of the free water surface inside the fluid reservoir are disregarded in this simplified first analysis. For positive tilt angles $\alpha > 0$ the righting moment M_y and arm RA_y should be negative to provide floating stability. If this is not the case, the tilt angle would increase until a new stable position is reached.

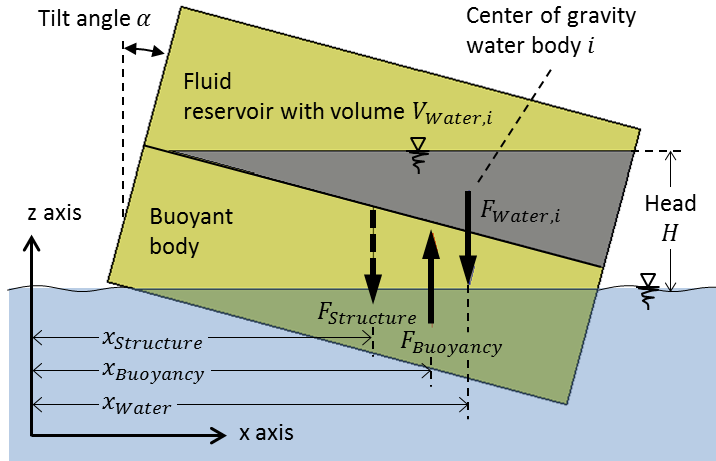


Figure 10. Schematic sketch of a floating box shaped basic 'light' BE system (according to Figure 1), the resulting forces F in vertical direction and their application points depending on the tilt angle α .

Exemplary two box shaped basic 'light' BE storage device (according to Figure 1) with rigid walls are analysed. To obtain extremal floating conditions the structure mass is set to a very low value. One single camber defines the fluid reservoir of the first exemplary design whereas the second exemplary design consists of two fluid reservoirs separated by a thin vertical wall (Figure 11, lower illustrations). Both designs share the following dimensions and characteristics:

- Squared base are $A = 50 \cdot 50 = 2500 \text{ m}^2$
- Structure height $h = 30 \text{ m}$
- Total volume of fluid reservoir $V_{Water} = h/2 \cdot A = 37000 \text{ m}^3$
- Energy storage capacity $W = h^2/4 \cdot A \cdot \rho_w \cdot g = 1,5 \text{ MWh}$
- Wall thickness $t = 10 \text{ cm}$
- Structure mass $m_{Structure} = 1105,2 \text{ kg} \rightarrow F_{Structure} = 10,74 \text{ kN}$

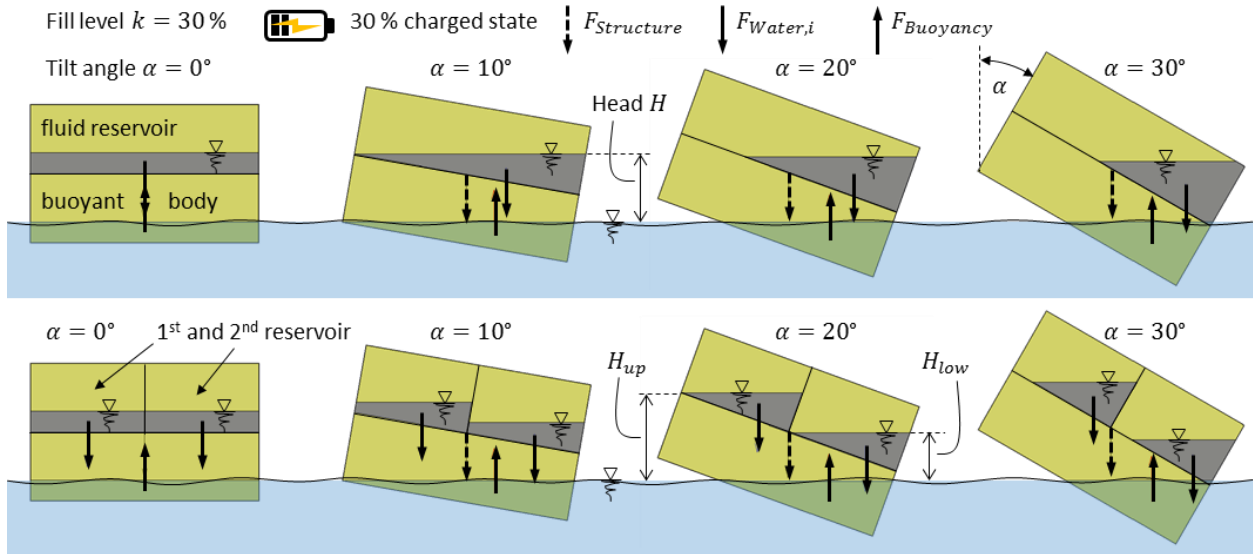


Figure 11. Floating position for several tilt angles α and a fill level $k = 30\%$. The top vertical cross-sections show the first exemplary design with one fluid reservoir. Right below the second exemplary design with two separated fluid chambers is illustrated.

Figure 12 shows the resulting righting arms RA_y and Figure 13 the pressure heads H for the first (left side) and second (right side) exemplary design. Obviously, one fluid reservoir leads to an unstable floating behavior whereas two separated fluid chambers represents a significant improvement. The second exemplary design is stable below fill levels $k < 70\%$. Especially for the basic 'light' BE concept the floating design requires strong efforts and additional measures to ensure floating stability.

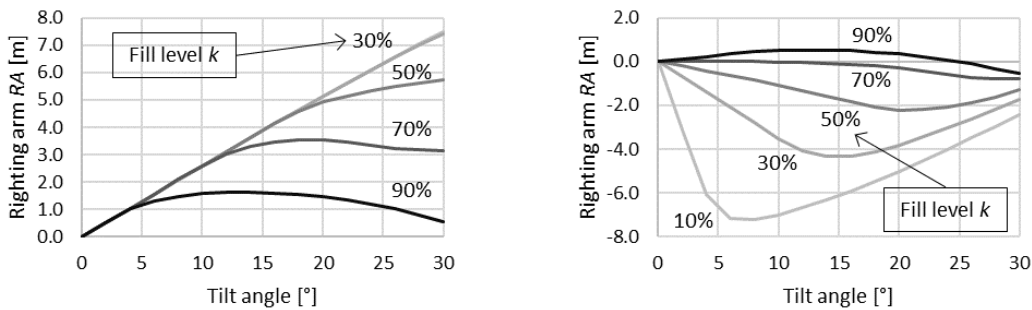


Figure 12. Righting arm RA_y over tilt angle α for different fill levels k . Left: first exemplary design. Right: second exemplary design.

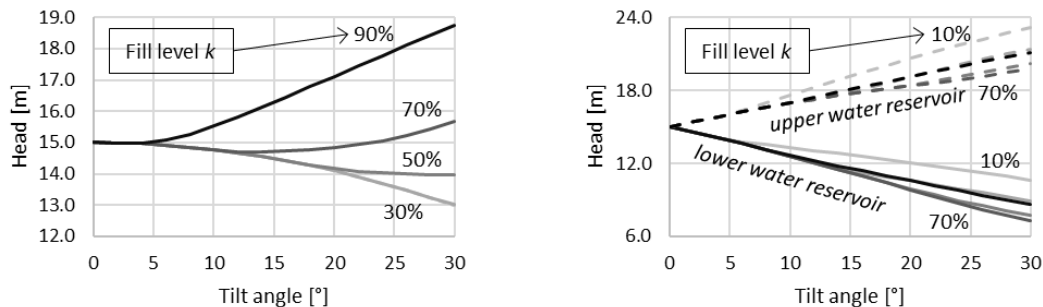


Figure 13. Head H over tilt angle α for different fill levels k . Left: first exemplary design. Right: second exemplary design showing two heads for the two separated fluid reservoirs (Figure 11).

5. Concluding Remarks and Outlook

Although, the development of BE structures composed of fabric is on a very early stage the presented theoretical results are promising. The intention of the design approaches of chapter 2 and 3 is to show the principal feasibility and to get indications for possible dimensions and the associated energy storage capacities. The energy storage capacity of the original ‘light’ and ‘heavy’ BE concepts could be increased significantly with the additional integration of forms of compressed air energy. However, the investigations all presuppose ideal conditions and isothermal processes. The increase of energy storage capacity goes hand in hand with large differences in power and head values along the charging and discharging process. These time invariant parameters require customized multi-stage pump-turbine solutions. Furthermore, the introduced design approaches show generally an increasing complexity compared to the original BE concepts. Especially for long-term applications, more simple solution with lower energy densities but with multi-use space on the platform roof (‘heavy’ BE system [6]) may be more successful.

The main motivation to think about storage solutions based on fabric is an expected decrease of construction costs compared with rigid structures and advantages for fabrication, packaging, shipment and deployment. A challenge for future research is to find a suitable fabric material, which fulfills the requirements summarized in chapter 2.4. and is cost-effective at the same time.

Due to the relatively high elevation of the centre of gravity compared to the center of buoyancy and the low structure weight, the floating stability for ‘light’ BE systems has to be considered carefully. Therefore, additional measures beside the floating body design may be required. Hydrodynamic forces and moments due to water sloshing arising from water oscillations in the fluid reservoir under wave or wind load may reduce the stability limit. The assessment of such effects and the development of anti-slosh measures are part of further studies.

To conclude Figure 14 shows finally a schematic visionary sketch, which aims to combine the design approaches, presented in chapter 2 and 3. This proposed BE system consists exclusively of fabric. The stabilizing fabric tubes are attached to each other for structural reinforcement. Openings or pipes between the air and water volumes of the stabilizing system allow fluid exchange. In addition, the stabilizing systems air volumes connect to the buoyant body in the center (umbilical connection, Fig. 14). Two hydraulic pump-turbine/motor-generator systems provide the energy conversion, one connected to the fluid reservoir in the center and the second to the stabilizing tubes.

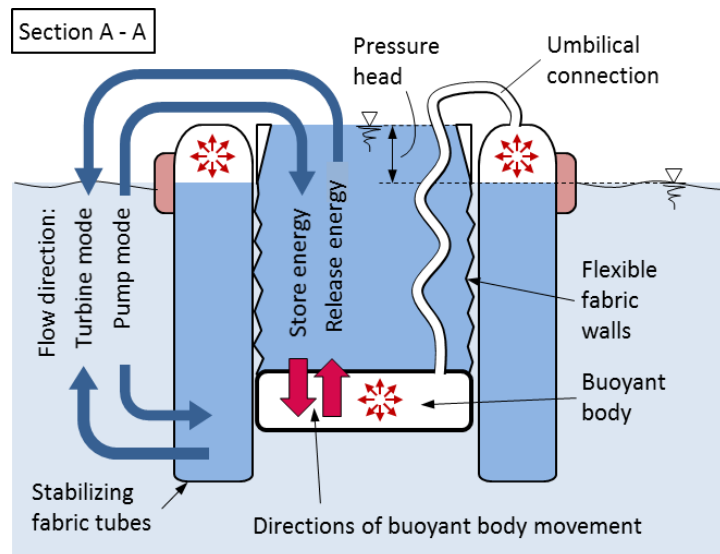


Figure 14. Schematic sketch of the proposed BE system of Figure 4 in combination with the design approach of chapter 3 using the stabilizing fabric structure as additional hydro-pneumatic storage possibility.

References

- [1] D. Buhagiar, T. Sant, Modelling of a novel hydro-pneumatic accumulator for large-scale offshore energy storage applications, *Journal of Energy Storage* (2017).
- [2] H. Henning, D. Hau, C. Dick, M. Puchta. Techno-economic assessment of a subsea energy storage technology for power balancing services, *Energy* (2017).

- [3] A. H. Slocum, G. E. Fennell, G. Dundar, B. G. Hodder, J. D. Meredith, M.A. Sager, Ocean Renewable Energy Storage (ORES) System: Analysis of an Undersea Energy Storage Concept, Proceedings of the IEEE 101 No. 4, 2013, pp. 906-924.
- [4] A. J. Pimm, S. D. Garvey, M. de Jong, Design and testing of Energy Bags for underwater compressed air energy storage, *Energy* 66, no. 1 (2014) 496-508.
- [5] M. Saadat, P. Y. Li, Modeling and Control of a Novel Compressed Air Energy Storage System for Offshore Wind Turbine, American Control Conference, 2012, pp. 3032-3037.
- [6] R. Klar, M. Aufleger, T. Sant, V. Neisch, R. Farrugia, Buoyant Energy – balancing wind power and other renewables in Europe’s oceans, Proceedings of Offshore Energy and Storage Symposium (OSES), 2015.
- [7] R. Klar, M. Aufleger, G. Scheide, V. Neisch, PrepareBE (Buoyant Energy) – exploratory project presentation, Proceedings of Offshore Energy and Storage Symposium (OSES), 2016.
- [8] University of Innsbruck, Unit for Hydraulic Engineering, Prepare Buoyant Energy – Entwicklung innovativer Konzepte zur hydraulischen Offshore Energiespeicherung mittels schwimmender Reservoirs (Proposal), Energieforschungsprogramm 2. Ausschreibung Sondierung; Österreichische Forschungsförderungsgesellschaft (FFG), 2015.
- [9] S. L. Veldman, Design and Analysis Methodologies for Inflated Beams, Doctoral thesis, Faculty of Aerospace Engineering, Delft University of Technology, Delft, Netherlands, 2005.
- [10] S.L. Veldman, O.K. Bergsma, A. Beukers, Bending of anisotropic inflated cylindrical beams, *Thin-Walled Structures* 43 No. 3 (2005) 461-475.
- [11] C. Wielgosz, J.C. Thomas, Deflections of inflatable fabric panels at high pressure, *Thin-Walled structures* 40 No.6 (2002) 523-536.
- [12] A. Le van, C. Wielgosz, Bending and buckling of inflatable beams: Some new theoretical results, *Thin-Walled Structures* 43 No. 8 (2005) 1166-1187.
- [13] I. Staffell, M. Rustomji, Maximising the value of electricity storage, *Journal of Energy Storage* 8 (2016) 212-225.